

Characteristics of Plume Releases as Depicted by Balloon Launchings and Model Simulations

R. A. STOCKER*, R. A. PIELKE*[†], A. J. VERDON** AND J. T. SNOW[‡]

*Cooperative Institute for Research in the Atmosphere, Fort Collins, Colorado

[†]Department of Atmospheric Science, Colorado State University, Fort Collins, Colorado

**National Center for Earth Science Education, American Geological Institute, Alexandria, Virginia

[‡]Department of Earth and Atmospheric Sciences, Purdue University, West Lafayette, Indiana

(Manuscript received 31 October 1988, in final form 14 July 1989)

ABSTRACT

On 12 May 1986, approximately 190 000 tagged helium balloons were released at 1330 EDT from locations scattered throughout the United States. An average of 4.5% of the balloon tags were recovered and sent to the American Geological Institute. A map of resultant balloon trajectories was then generated from the data. From an analysis of the surface and 500 mb maps on this data, synoptic conditions are defined and categorized. This along with the resultant motion map gives useful data for identifying the dispersion characteristics involved with a particular synoptic condition.

The ARL-ATAD model, a single-layer trajectory model, was run for the 12 May balloon launch for a PBL and 750-660 mb layer simulation from seven sites across the United States. These were compared with the balloon resultant motion map. The PBL approach produced poor comparisons with two of the seven sites showing balloon and trajectory motions transporting plumes in opposite directions. The layer approach did much better with only the Los Angeles, California comparison showing disagreement. Yet even with the layer approach, the ability of the ATAD model to predict plume transport is highly questionable due to the lateral dispersion evidenced by the balloon resultant motions.

This experiment is of great interest because of the uniqueness involved with the spatial extent and total number of released balloons.

1. Introduction

The question of the contribution of long-range versus local transport to the aerosol loadings observed at various sites has been debated for many years. Long-range transport models are one tool which has been used to address this question, however, problems arise because all current Environmental Protection Agency (EPA) and National Park Service (NPS) transport models include only large-scale synoptic effects (10-1000 km) and fail to incorporate smaller scale mesoscale influences (10-10 000 m). Over complex and inhomogeneous terrain, these effects have been shown to be significant in altering pollution transport patterns (e.g. Moran et al. 1986). This can lead to erroneous conclusions when trying to determine the contribution of a source to a particular receptor's aerosol emission.

The current study is used to help in determining when a commonly used single-layer transport model can simulate the "real" atmospheric transport and when it cannot. In this study, a large number of helium-filled balloons were released from diverse locations

across the United States under a variety of synoptic conditions. The transport model was then run using simulated releases from several of the balloon origin locations and examined to see if the model could adequately explain the observed displacement of the balloons.

2. Experiment description

a. Balloons

On 12 May 1986, as a part of National Science Week, close to 190 000 helium-filled latex balloons were released by school children at over 800 sites around the United States. The balloons were scheduled to be released simultaneously at 1330 EDT from all the sites after being inflated to a diameter of 9 inches.

The number of balloon releases from any given area was determined solely by the willingness of a school to participate; as might be expected, larger population centers tended to have more releases. A tag was attached to each balloon giving origin information and the address of the American Geological Institute (AGI) for returning the tag after it had been recovered from a downed balloon. Each tag contained a section for the finder of the balloon to complete which identifies where the balloon was found. Approximately 4.5% or 8000

Corresponding author address: Mr. Roger Stocker, Department of Atmospheric Science, Colorado State University, Fort Collins, CO 80523.

of the tags were recovered and sent to AGI for collection. The tags were then forwarded to Colorado State University where they were coded into origin/endpoint latitude and longitude pairs. A simple quality control check to eliminate anomalously long path distances and boundary errors (i.e., endpoint location over the oceans) was run on the origin/endpoint pairs after they were digitized.

To help in clarifying some of the unknowns evidenced with an experiment of this kind, a study was conducted at West Lafayette, Indiana. Two test cases involving helium-filled latex balloons, one on 18 July 1987 and the other on 12 September 1987, were initiated in prefrontal conditions with characteristic strong winds aloft and little vertical directional wind shear. This synoptic condition would be expected to produce the least amount of horizontal dispersion of any of the synoptic classifications presented in this paper. Coupled with the field experiment, an empirical formula was developed that attempted to simulate balloon flight paths based on a single NWS rawinsonde station upwind of the release point. Controlled balloon releases at Purdue University were used in obtaining the initial rise rates of the balloons and were found to be in a range from 1.2–1.8 m s^{-1} .

The balloon release on the morning of 18 July 1987 involved releasing 106 balloons of which 15 were recovered. All balloons were inflated to 12 inches in diameter over a 20-minute period and then released simultaneously shortly thereafter to produce a uniform launch. The recovered balloons mapped out a fairly tight clustering 100 km from the release point with a travel time of about three hours. Although a fairly tight clustering is evident on average, the total area covered by the balloons exceeds 4400 km^2 . The model simulation (based on the empirical formula) of the transport path produced good agreement with the balloons using initial rise rates from 1.2–1.8 m s^{-1} . These rise rates simulate differences in balloon diameter.

The balloon release on the morning of 12 September 1987 involved 21 balloons with 3 being recovered. Again, the balloons were inflated to 12 inches in diameter, but the gas was allowed to diffuse through the latex skin for two hours prior to release thus producing irregularities in rise rates. Of the three balloons recovered, two were found within 8 km of each other at a distance of about 75 km from the origin. The remaining balloon was found 250 km from the origin along the same flight line as the other two.

The results of the Purdue study suggest that there is a significant increase in the dispersion pattern of the balloons that were released directly after inflation versus those for which helium gas was allowed to diffuse through the latex skin for two hours prior to release. This last scenario, which quite probably happened to some extent with the 12 May balloon launch, could explain some of the dispersion represented in the 12

May release, but as suggested by the Purdue experiment, there is still significant dispersion in a prefrontal synoptic condition with an instantaneous release.

b. Trajectory model

The National Oceanic and Atmospheric Administration Air Resource Laboratories Atmospheric Transport and Dispersion model (ARL-ATAD) is used in the current study in order to compare with the observed balloon dispersion. The ARL-ATAD model will be described only to the extent needed for clarification of its use in this study; further explanation of the model can be found in Heffter (1980).

The ATAD model is a single layer trajectory model which uses layer-averaged winds to obtain estimates of parcel transport. The layer-averaged winds for a trajectory segment are calculated using rawinsonde information within a 480 km radius from the origin of the segment. The winds are averaged vertically between an average terrain height (ATH) and a "critical inversion" height. As an alternative to using the critical inversion criteria, the model also has the capability to calculate a different layer-averaged wind by predefining a vertical layer above the ATH and then averaging the winds within this layer.

The critical inversion is defined as an atmospheric layer having a potential temperature lapse rate of 5°C km^{-1} or more with the potential temperature at the top of the inversion being 2 degrees higher than at the base. The ATH is based on the elevation of the region around the rawinsonde station. The rawinsonde data is weighted as a function of R^{-2} where R is the distance from the segment origin to the station. The transport layer depth (TLD) for averaging the winds is defined as the average inversion height minus ATH but always falls within the range $300 \text{ m} \leq \text{TLD} \leq 3000 \text{ m}$ above the ATH. For a forward trajectory run at night, there is also a correction to reduce the TLD based on the assumption that the boundary layer will be reduced in height at night, but because of the shallowness of the nighttime inversion, the critical inversion criterion will not be met. After the TLD has been obtained, the layer-averaged wind is computed and used in the calculation of a 3-hour trajectory segment. The model is capable of producing up to four trajectories per day for five days in duration, with trajectory segments every three hours.

The ATAD model has been tested against other more complex multilevel models (Bresch et al. 1984), similar single-level models with tetrons (Clarke et al. 1983; Reisinger and Mueller 1983), and an isentropic trajectory model (Artz et al. 1985). In most cases, the ATAD model showed good agreement with other transport models except in areas of large baroclinicity, precipitation or synoptic patterns dominated by light and variable synoptic flows. Studies have also been

TABLE 1. Overview of meteorological aspects of the four synoptic categories that can be directly obtained from synoptic surface analyses (Northern Hemisphere) (adapted from Forbes and Pielke 1985; and Pielke et al. 1987).

Characteristics	Category			
	1	2	3	4
Category class	mT; in the warm sector of an extratropical cyclone	mT/cP, mT/cA, mP/cA; ahead of the warm front in the region of cyclonic curvature at the surface	cP, cA; behind the cold front in the region of cyclonic curvature to the surface isobars	cP, cA; under a polar high in a region of anticyclonic curvature to the surface
Surface winds	Brisk SW surface winds	Light to moderate SE to ENE surface winds	Strong NE to W surface winds	Light and variable winds
Vertical motion	Weakening synoptic descent as the cold front approaches	Synoptic ascent due to warm advection and positive vorticity advection aloft	Synoptic ascent due to positive vorticity advection aloft (in this region this ascent more than compensates for the descent due to cold advection)	Synoptic descent (due to warm advection and/or negative vorticity advection aloft)
Inversion	Weak synoptic subsidence inversion caps planetary boundary layer	Boundary layer capped by frontal inversion	Deep planetary boundary layer	Synoptic subsidence inversion and/or warm advection aloft create an inversion which caps the planetary boundary layer
Dominant mesoscale systems	Squall lines	Embedded lines of convection	Forced airflow over rough terrain systems; lake effect storms	Mountain-valley flows; land-sea breezes; urban circulations (thermally-forced systems)
Ventilation	Moderate to good ventilation	Poor ventilation of low level (i.e. below frontal inversion) emissions	Excellent ventilation	Night or snow-covered ground: poor ventilation; day: poor to moderate ventilation
Deposition	Dry deposition except wet deposition in showers	Dominated by wet deposition	Dry deposition except in showers	Dry deposition
Transport	Long range	Long range above inversion	Long range	More local as you approach the center of the polar high

done to identify errors in the ATAD trajectory endpoint locations (Raynor et al. 1983; Sheih 1983; and Kuo et al. 1985), showing that use of a different velocity interpolation scheme and increased temporal resolution of sounding data would cause significant improvement in the ATAD model trajectory results. Also, smoothing of the wind fields by the ATAD model underestimates the lateral movement of a plume creating serious directional errors in some synoptic cases.

c. Synoptic classification

Synoptic-scale meteorological regimes can be categorized based on a subjective classification scheme first developed by Lindsey (1980). Table 1 gives an example of the classification used in this study. Category 1 is identified as the region ahead of a cold front characterized by brisk southwest surface winds, weak synoptic descending motion with an associated weak inversion and good ventilation. Category 2 is identified as the area ahead of a warm front characterized by light to moderate southeast to east-northeast winds, synoptic ascent and poor low-level ventilation. Category 3 is identified as the area behind a cold front characterized

by strong northeast to west surface winds and excellent ventilation. Category 4 is identified as the region under a cold core anticyclonic high pressure characterized by synoptic descent, a strong subsidence inversion with

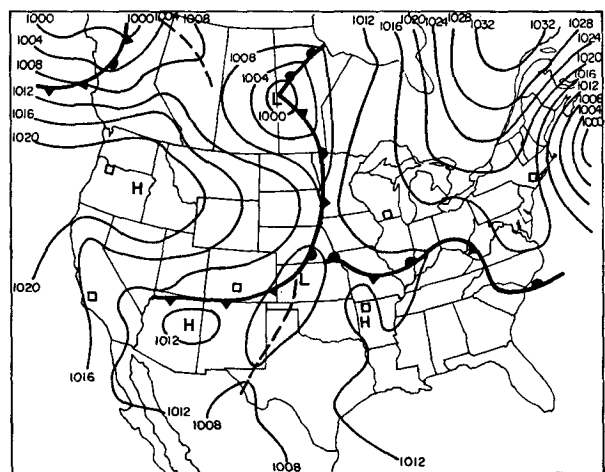


FIG. 1. Surface weather map for 0700 EDT 12 May 1986. ATAD trajectory origin locations are indicated by squares.

light surface winds in the interior of the high pressure and poor ventilation.

Figure 1 shows the surface weather map and ATAD origin locations for the morning of the 12 May 1986 balloon launch. Sections of the country dominated by a polar high (category 4) include the Pacific Northwest, the southeastern sections of the United States along with portions around the Great Lakes. Areas behind the cold front (category 3) include regions of the intermountain west and northern Great Plains and all along the northern part of the East Coast. Sections identifying precold frontal situations (category 1), include parts of Oklahoma, Kansas and Texas.

3. Results

a. Balloon dispersion

Balloon resultant motion for the 12 May 1986 launch can be seen in Figs. 2 and 3. The high density of data east of the Rockies is likely due to the number of people in the experiment. West of the Rockies, the limited amount of data could be due to reduced population density in either or both the original and end-point locations.

As an overall observation, it is relatively simple to examine Fig. 2 and be able to distinguish areas dominated by particular types of weather systems. In the northern intermountain region of Colorado, Wyoming and Nebraska, the large northeast displacement corresponds to the southwest winds aloft just behind a cold front (category 3). In the area around Texas and Mississippi, indications of a strong-wind polar high (category 4) with a well-defined large-scale wind can be seen in the anticyclonic path of the balloons. Another polar high can be located around the Great Lakes area; this area is typical of a category 4 with lighter winds and large directional wind variability. On the East Coast, the area behind the back-door cold front

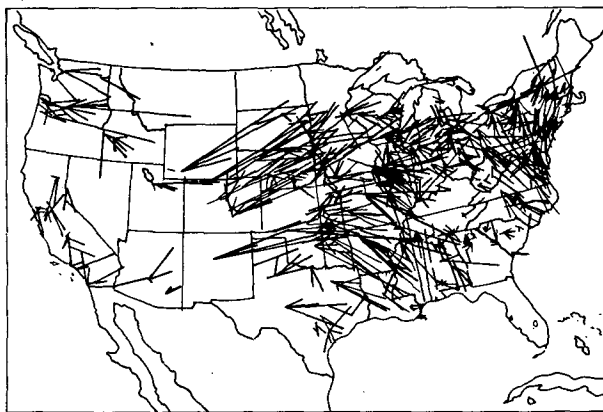


FIG. 2. Resultant motion for the 12 May 1986 balloon launch.

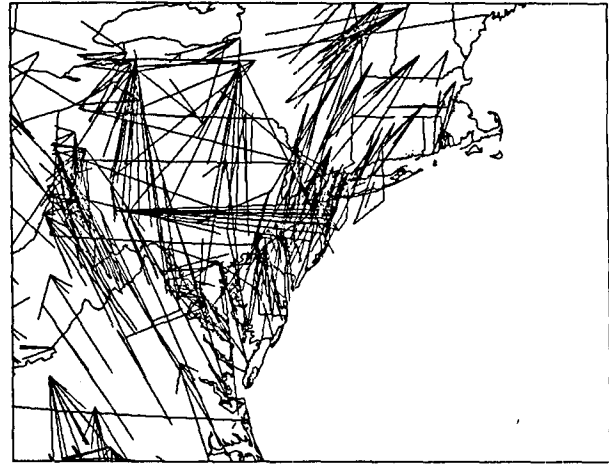


FIG. 3. Balloon dataset for the East Coast.

(category 3) can clearly be identified in Fig. 3 by the cyclonic path of the balloons.

Comparing Figs. 1 and 2, it can be seen that the balloon paths were frequently different than what would be implied by the pressure gradient on the surface map. It appears, therefore, that the balloons were transported at an equilibrium altitude higher than the near surface elevation. After examining the 850, 700 and 500 mb maps for the time of the balloon release, it was concluded that the 700 mb gradient flow traced out a similar pattern to that of many of the balloon paths. One might also think to use the initial rise rates and empirical formula developed in the Purdue case to see if the 700 mb level was a reasonable estimate for an equilibrium transport level, but since this formula is very sensitive to the flight duration of a balloon, known only by estimation to be less than a day, the empirical formula was not used in this paper to substantiate this equilibrium transport level.

b. Site comparisons

To examine the balloon dataset in greater detail, six sites across the United States were chosen to compare both the balloon paths and the ATAD trajectories. National Meteorological Center (NMC) rawinsonde data were also collected for each of the six launch positions for all locations used in the calculation of a trajectory segment. To conserve space in this article, only the closest one is shown in the following figures. ATAD origins were selected based on obtaining a representation of the model behavior in the differing classification regions and the amount of balloon data available. The following six locations were chosen as ATAD origins: Madison, Wisconsin; Portland, Oregon; Los Angeles, California; New York, New York; Rogers, Arkansas; and Denver, Colorado.

The ATAD model was run for each of the six sites

for a duration of 48 hours. From balloon-tag recovery times and average 700 mb wind speeds, it appears that most balloon flight durations were less than one day. Two ATAD model runs were made per site. The first involved an average wind calculation based on rawinsonde data which calculated a critical inversion height. The second run involved the computation of an averaged wind around 700 mb. (The 750–660 mb layer was chosen.) The first run is referred to as the Planetary Boundary Layer (PBL) experiment; the second is referred to as the Constant Layer Run (CLR).

The two models runs (PBL and CLR) were made to demonstrate potential problems with using the ATAD model to simulate transport of an aerosol/gas plume released from a point source (i.e., coal-fired power plant) with some initial buoyancy characteristics due either to temperature or velocity considerations. The fact that both the balloons and an aerosol/gas plume emitted from a stack are initially buoyant are used in this paper to obtain qualitative estimates of plume behavior based on balloon resultant motion. This does not mean that the trajectories of a balloon and pollutant plume are assumed to be identical, but only that since both are initially buoyant that the buoyancy factor of a pollutant plume can be tested qualitatively by the balloon resultant motions.

The PBL approach represents the most common application of the ATAD model because of its easy automation capability. When this approach is applied to a point-source plume as mentioned above, however, there are many scenarios that can be presented which would indicate that the ATAD model would do a poor job in obtaining a trajectory that would closely follow the pollutant plume. One possible scenario would be that the plume had sufficient buoyancy to rise to a greater depth than the TLD and thus the transport winds might be different than those obtained from the ATAD model using the PBL approach.

The CLR approach is expected to be a more realistic approach but it is not currently automated since one needs to input the transport layer in which the plume is neutrally buoyant prior to the run. Therefore, although one would expect better trajectory agreement with the CLR approach, especially in highly sheared environments, the loss of the automation feature is a serious drawback.

Figure 4a shows a comparison between the ATAD model and the balloons for Madison, Wisconsin. The narrow, solid lines represent the balloon resultant displacement and the solid, bold lines represent the ATAD trajectories computed from the PBL and CLR calculations. Perpendicular tick marks across the ATAD trajectories indicate 3-hour segment end points. The solid square represents the ATAD origin location and the solid circles show the placement of the nearest rawinsonde station used in computing the ATAD trajectories.

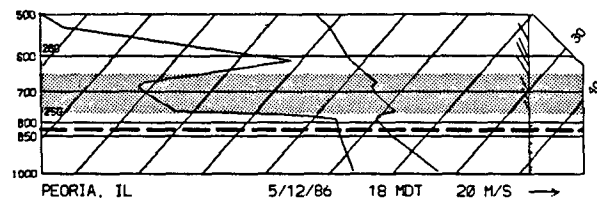
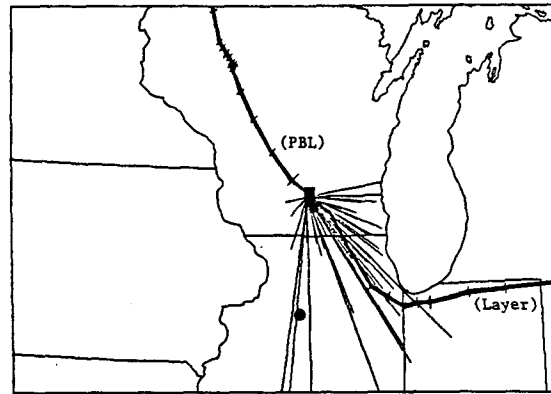


FIG. 4. Comparison of balloon and ATAD results for a light wind category 4 situation (a) PBL and layer trajectories along with balloon resultant motion from Madison, Wisconsin (solid square represents ATAD origin, solid circle represents nearest sounding), and (b) nearest sounding site at 1400 EDT for Peoria, Illinois with the 750–660 mb layer shaded and the transport layer height (TLH) of 825 mb indicated by the dashed line.

The area around Madison, Wisconsin is dominated by a category 4 polar high with light winds. The balloon flow clearly shows an approximately 180-degree fan in the balloon endpoints. Thus, the ability of any synoptic-scale single trajectory model to predict long-range or even short-range transport for this synoptic situation is questionable. The ATAD trajectory computed for the PBL case heads off in a northwest direction. From the sounding in Fig. 4b from Peoria, Illinois, it can be seen that no winds would transport a plume in this direction. However, a sounding from Green Bay, Wisconsin for the same time indicates geostrophic south to southeast winds of 5 m s^{-1} from the surface to 1500 m. This trajectory path is inconsistent with the balloon motions.

The CLR calculation shows a trajectory simulating several of the balloon paths. Although this result seems to predict an average transport well, the individual paths of each balloon are also important with respect to dispersion. In addition, when there is a large fanning of the balloon paths, the significance of a “mean” trajectory is small. The Peoria, Illinois sounding for the 750–660 mb layer has strong north to northwest winds of $\geq 10 \text{ m s}^{-1}$. The Green Bay, Wisconsin sounding

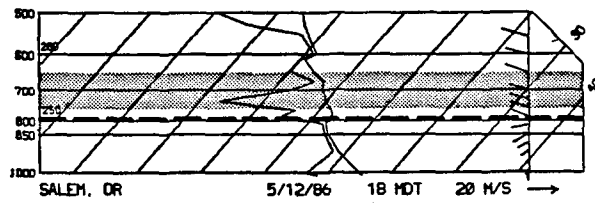
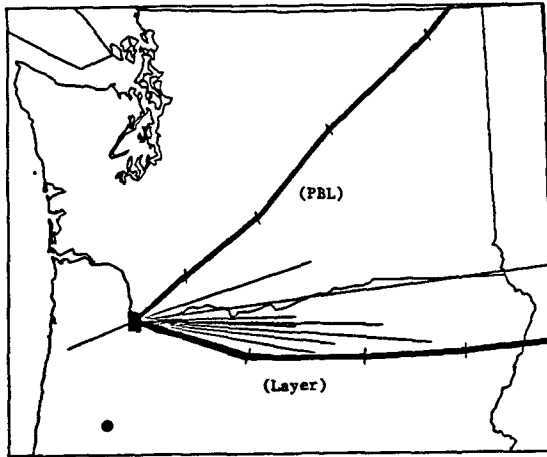


FIG. 5. Comparison of balloon and ATAD results for a category 4 strong wind situation (a) PBL and layer trajectories along with balloon resultant motion from Portland, Oregon (solid square represents ATAD origin, solid circle represents nearest sounding), and (b) nearest sounding at 1700 EDT for Salem, Oregon with a TLH of 790 mb.

also has northwest winds in this layered region but the maximum wind speeds reach only about 5 m s^{-1} . By examining the 3-hour tick marks from the CLR trajectory, the transport time indicates durations of balloon lifetimes on the order of one day.

Figure 5a shows another comparison region dominated by the northern part of a polar high (category 4). The influence of an occluded front is seen to affect the northern section of Washington and on towards the north through British Columbia, Canada. Balloon releases from the Portland, Oregon site resulted in the movement of the balloons toward the east apparently through the Columbia River gorge, which is a canyon splitting the Cascade mountain range between Oregon and Washington. Figure 5b shows the closest sounding station, Salem, Oregon, about 90 km to the south of Portland. The sounding shows the high humidity coastal air of the Willamette Valley with very little vertical directional wind shear. The wind is predominately from the west except for a small segment from ground level to 1 km above the surface where the wind is from the southwest. This flow at the surface is why the ATAD

PBL run predicts parcels to initially move toward the northeast. With the CLR approach, after initial southeasterly movement because of the winds within the transport layer, the ATAD model predicts a direct easterly track. Examining the tick marks of the CLR ATAD run, it can be seen that these strong west winds ($\geq 10 \text{ m s}^{-1}$) indicate that balloon flight times were less than nine hours.

Figure 6a once again shows an area dominated by a polar high (category 4). The Los Angeles, California region encompasses a large urban area enveloped in highly complex terrain. For many years, The Los Angeles Basin has been a controversial area with respect to long-range transport and has been blamed for much of the regional haze that occurs in the southwestern United States. As with the Madison, Wisconsin example, light synoptic winds produce no dominant directional wind transport with 180 degrees of variability evident. There is also the possibility of an even greater

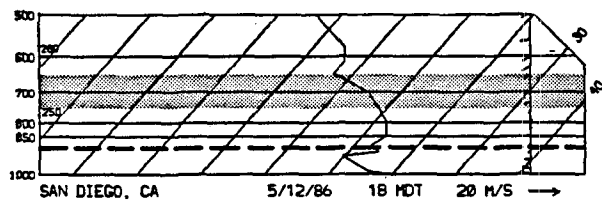
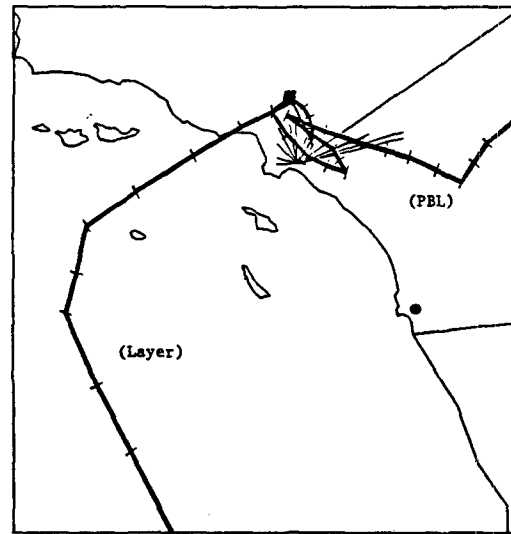


FIG. 6. Comparison of balloon and ATAD results for a light wind category 4 situation (a) PBL and layer trajectories along with balloon resultant motion from Los Angeles, California (solid square represents ATAD origin, solid circle represents nearest sounding), and (b) nearest sounding site at 1700 EDT for San Diego, California with a TLH of 910 mb.

spread because of transport into the Pacific Ocean, due to a sea breeze circulation, where balloons would not be retrieved. The balloon paths are confined to the Los Angeles Basin except for one which travels towards the northeast and Las Vegas, Nevada. There could be two explanations for the majority of the balloon segments ending in the basin: light winds and a PBL below the mountains surrounding the basin trapped the balloons, and/or because east of the mountains surrounding the basin, there is an arid, sparsely populated desert, which would result in a small return of balloon tags that happened to fall in the region.

Figure 6b shows the nearest rawinsonde station at San Diego, California. A strong low-level inversion can be seen at 900 mb. The winds up to 2500 m above the surface are light ($\leq 2.5 \text{ m s}^{-1}$) and variable. In this case, the PBL trajectory representation of the balloon resultant motion is better at following the balloon resultant path than the trajectory computed by the CLR. The PBL and CLR simulations initially tend to stay

within the basin region showing a surprising recirculation pattern. After this initial time, the two simulations diverge with the PBL trajectory heading off to the east and the CLR trajectory simulating transport over the oceans.

Figure 7a shows the East Coast region which was dominated by cyclonic isobaric curvature behind a back door cold front (category 3). From this figure and that of Fig. 3, there is the indication of a general tendency for the balloons to be carried in a cyclonic flow down the East Coast. From Fig. 7a, the longer distance balloon resultant paths support this flow direction, but the shorter resultant paths appear to be dominated by mesoscale flows as evidenced by the motions towards the north and east. However, the PBL ATAD trajectory simulates anticyclonic transport, indicating the influence of the high pressure region in southeastern Canada. The CLR approach seems to suggest transport of the balloons along the back-door cold front. Figure 7b shows a sounding from Atlantic City, New Jersey with low level easterlies of 6 m s^{-1} that produced westerly movement of the PBL trajectories. The CLR case included stronger northwest and northeasterly winds ($7\text{--}12 \text{ m s}^{-1}$) that produced the southerly simulated trajectory movement.

Because of the large number of rawinsonde stations affecting the calculation of each ATAD trajectory segment in the eastern United States—five to six on the East Coast compared with one or two in the west—a test of the ATAD model was conducted to determine the sensitivity of the model to the initial model origin as a result of a large number of input data stations. To do this, along with the New York model run, an ATAD simulation was also made at Williamsport, Pennsylvania, a few hundred kilometers to the west with both model runs using the PBL approach. Results showed that there was little change in the simulated ATAD trajectories for Williamsport when compared with those of New York.

Figure 8a shows another category 4 situation. In this figure, balloons were released from the following cities: Nevada, Missouri; Rogers, Arkansas; and Wickes, Arkansas with the ATAD model initiated from Rogers, Arkansas. This is a region dominated by a higher wind speed category 4 with a stationary front to the north. The PBL case predicts transport of a parcel initially to the north which is contrary to the pattern of southeasterly movement by the balloons. The CLR calculation is once again better at estimating the balloon resultant flow with more of a south to southeast transport. The lateral dispersion in this figure is only 5–15 degrees of arc with both the Nevada, Missouri and Wickes, Arkansas balloon motions showing a greater degree of lateral variability than the Rogers, Arkansas site. Figure 8b represents the Monett, Missouri rawinsonde site to the north of the ATAD origin. The lower wind up to 1400 m above the surface has mostly a southerly com-

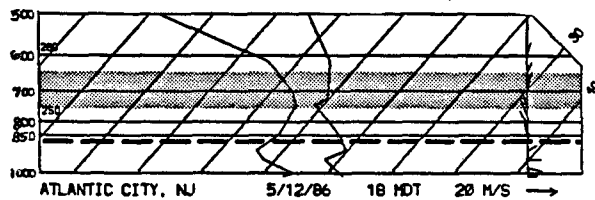
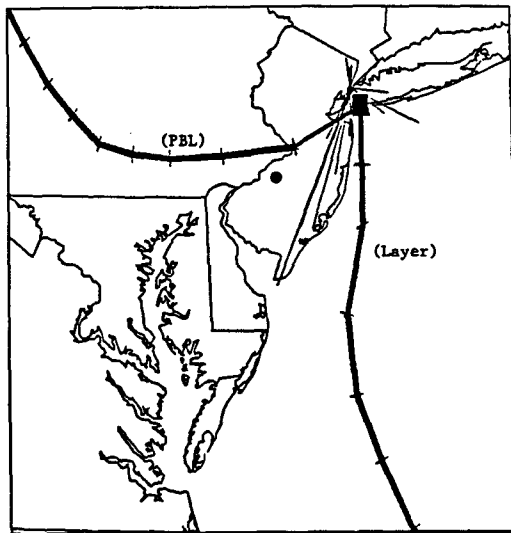


FIG. 7. Comparison of balloon and ATAD results for a category 3 situation (a) PBL and layer trajectories along with balloon resultant motion from New York, New York (solid square represents ATAD origin, solid circle represents nearest sounding), and (b) nearest sounding at 1700 EDT for Atlantic City, New Jersey with a TLH of 862 mb.

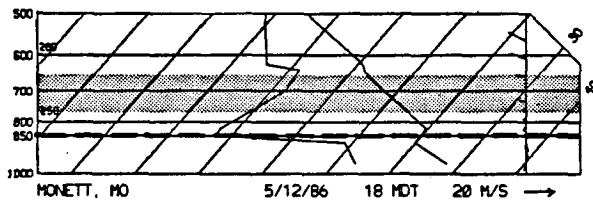
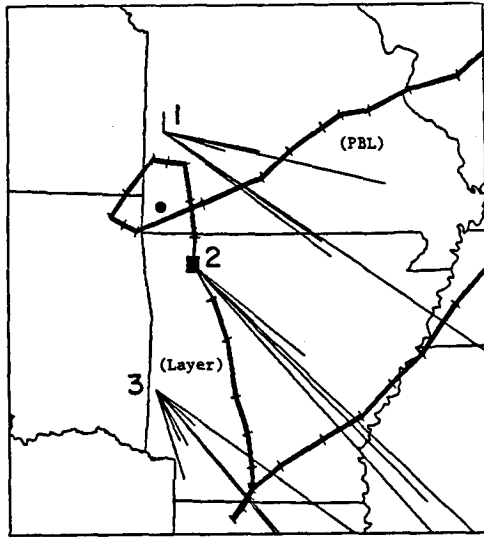


FIG. 8. Comparison of balloon and ATAD results for a category 4 strong wind situation (a) PBL and layer trajectories for Rogers, Arkansas with associated balloon motion from three sites: 1) Nevada, Missouri, 2) Rogers, Arkansas, and 3) Wickes, Arkansas (solid square represents ATAD origin, solid circle represents nearest sounding), and (b) nearest sounding at 1700 EDT for Monett, Missouri with a TLH of 850 mb.

ponent evidenced by the northward movement of the PBL trajectory initially. The Monett, Missouri wind profile does not show any evidence of a southerly component to support the CLR trajectory, but the wind profile at Little Rock, Arkansas to the southeast of Rogers, Arkansas, clearly shows a strong vertical band of northwesterly winds from the surface up to 5000 m.

Figure 9a shows a region in Colorado. This region is under a category 3 situation with large mixing depths, strong winds, and large directional wind changes with height. Four balloon sites are used to compare with the one ATAD site. The ATAD origin site is a few hundred kilometers to the south of the closest balloon release site, but as has been shown previously, with a synoptic-scale transport model there should be no appreciable difference in results due to this displacement. The four balloon sites were chosen to show any difference between sites west and east of the Rocky Mountains with the two most western sites representing the

western side and the other two the eastern side of the mountain barrier. In general, the balloon resultant motion field tends to exhibit transport toward the north or northeast. The only difference between the east and west balloon paths seems to be a higher amount of lateral dispersion in the ones released in the east. The PBL and CLR ATAD simulations show considerable similarity in this comparison because with Colorado's high elevation, the PBL and 750–660 mb layer represent almost the same layer and thus both calculations are similar wind profiles in the computation of the layer-averaged wind. Figure 9b (the sounding from Denver, Colorado) shows the overlap used by both calculations in obtaining a layer-averaged wind with the dominant wind direction being southwesterly.

4. Conclusions

The work involved in generating this study has served to both introduce this new dataset and gain further insight into the problems associated with using trajectory models based on rawinsonde data alone in determining long-range transport. Results from this study are outlined below.

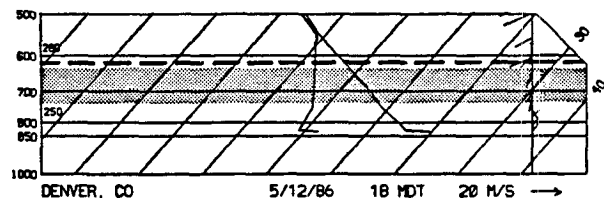
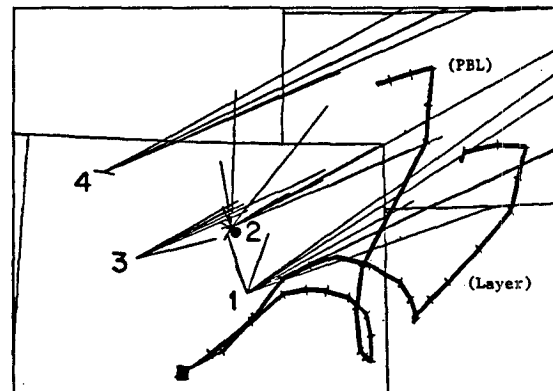


FIG. 9. Comparison of balloon and ATAD results for a category 3 situation (a) PBL and layer trajectories for Alamosa, Colorado with associated balloon motions from four sites: 1) Colorado Springs, Colorado, 2) Denver, Colorado, 3) Aspen, Colorado, and 4) Craig, Colorado (solid square represents ATAD origin, solid circle represents nearest sounding); and (b) nearest sounding at 1700 EDT for Denver, Colorado with a TLH of 625 mb.

(i) The balloon paths suggested very distinct motions associated with each of the differing categorized synoptic regions. The light-wind category 4 polar high areas (Los Angeles, California and Madison, Wisconsin) produced balloon resultant paths which had no conclusive directional transport, but produced a fanning of at least 180 degrees in direction. As the polar high regions were positioned closer to a polar front (Portland, Oregon and Rogers, Arkansas), there was a tendency for the horizontal directional wind fan to become more focussed, creating a better defined transport wind. The eastern United States back-door cold frontal area produced an extensive region of cyclonically curved flow across the Northern Atlantic states. The horizontal directional shear was large in the New York comparison, which could be associated with mesoscale circulations due to land/ocean contrasts and the large urban area. From the Purdue experiment, prefrontal conditions suggested a small but significant amount of dispersion from the balloons resultant motions.

(ii) Comparison of the ATAD model with the balloon resultant motions for the PBL approach did poorly. In some cases (Madison, Wisconsin and Rogers, Arkansas), the balloon and trajectory motions were in complete disagreement. The only good comparison with the trajectory balloon motions came at the Colorado site where the layer-averaged winds computed for the PBL and CLR approach were similar. This does not necessarily mean that the PBL approach would do badly in all but one of the synoptic regimes, but it does suggest that since an aerosol/gas plume has an initial buoyancy, the plume might lift to a nonbuoyant equilibrium level above the PBL layer and thus be transported by a different transport wind than would be obtained by using the ATAD model and the PBL approach.

(iii) Comparison of the ATAD model and balloons for the CLR calculation (750–660 mb) were more accurate for the mean directional transport of the balloons than the PBL simulations although the spread of the balloons cannot be inferred from the single CLR ATAD model the way it was used. The only region where the ATAD model and balloons were not consistent in at least the general direction of movement was in the highly complex terrain surrounding the Los Angeles Basin. In this region, model predictions transported parcels over the Pacific Ocean while balloon resultant flow indicated a stagnation event with all but one of the resultant segments staying within the Basin. This stagnation apparently occurred because of the low PBL (914 m) and light winds ($\leq 3 \text{ m s}^{-1}$) with the mountain ranges to the east, north and south having elevations much greater than the PBL. This example effectively illustrates one of the biggest problems of the ATAD model which is that the transport layer depth in the model cannot be less than 300 m above the surface

and thus the flow can never be blocked completely (i.e., no stagnation events).

(iv) The maximum horizontal and vertical directional wind shear occurred under the category 4 light wind situations. This again demonstrates the difficulty in using synoptic models under light wind conditions in which mesoscale circulations (i.e., lake/land breezes, mountain/valley circulations etc.) are important. But even in the best case, the Colorado postfrontal example, the balloon transport directions still demonstrated directional variability of 10 degrees or more. Although this is quite small compared with the 180 degree variation produced in the light-wind category 4 synoptic cases, its relative impact upon long-range and, to a smaller extent, short-range pollution transport is of major importance. It clearly illustrates a major shortcoming of objective analysis trajectory models to simulate pollution transport and thus obtain relevant information about source attribution. For although trajectory models, at best, can simulate center of mass movement of pollution, as this study suggests, much of the pollutant mass would be associated with areas well removed from the center of mass trajectories.

This experiment, of course, can be looked at only from a qualitative viewpoint because of the many assumptions that have to be made (i.e., zero buoyancy balloons, simultaneous releases etc.). Nevertheless, this balloon dataset and ATAD model comparisons have been used to learn more about the question of long-range transport in hopes of developing better ways of attaining source attribution contributions. Among the major results are some guidelines for when the ATAD model is a realistic trajectory assessment tool and when it is not.

Acknowledgments. Funding for this work has been provided for in part by Electric Power Research Institute Contract RP-1630-53 and in part by National Park Service Contract NA81RAH00001, Amendment 17, Item 15. Model computations were performed on the Colorado State University CYBER 835 computer. Thanks are due to Thomas McLeland, Shawn Harley, and Mark Conner who helped with the Purdue balloon release, Judie Sorbie for drafting some of the figures and Dallas McDonald for typing and editing. We also would like to recognize the Triangle Coalition for Science and Technology Education and the many school children and teachers who made this unique scientific evaluation possible.

REFERENCES

- Artz, R., R. A. Pielke and J. Galloway, 1985: Comparison of the ARL-ATAD constant level and the NCAR isentropic trajectory analysis for selected case studies. *Atmos. Environ.*, **19**, 47–63.
- Bresch, J. F., L. L. Ashbaugh, T. Henmi and E. R. Reiter, 1984: Comparison of a single layer and a multi-layer transport model for residence time analysis. *Preprints 77th Annual Air Pollution Control Association Meeting*. San Francisco.

- Clarke, J. F., T. L. Clarke, J. K. S. Ching, P. L. Haagenson, R. B. Husar and D. E. Patterson, 1983: Assessment of model simulation of long-distance transport. *Atmos. Environ.*, **17**, 2449-2462.
- Forbes, G. S., and R. A. Pielke, 1985: Use of observational and model-derived fields and regime model output statistics in mesoscale forecasting. *Nowcasting Symposium at the IAMAP/IAPSO Joint Assembly*, Honolulu, *ESA J.*, 207-225.
- Heffter, J. L., 1980: Air Resources Laboratory Atmospheric Transport and Dispersion Model (ARL-ATAD). NOAA Tech. Memo. ERL-ARL-81.
- Kuo, Y. H., M. Skumanich, P. L. Haagenson and J. S. Chang, 1985: The accuracy of trajectory models as revealed by the observing system simulation experiments. *Mon. Wea. Rev.*, **113**, 1852-1867.
- Lindsey III, C. G., 1980: Analysis of coastal wind energy regimes. M.S. thesis, Department of Environmental Science, University of Virginia.
- Moran, M. D., R. W. Arritt, M. Segal and R. A. Pielke, 1986: Modification of regional-scale pollutant dispersion by terrain-forced mesoscale circulations. Proc., Second *Air Pollution Control Association Specialty Conf. on Meteorology of Acid Deposition*, Albany, 136-157.
- Pielke, R. A., M. Garstang, C. Lindsey and J. Gusdorf, 1987: Use of a synoptic classification scheme to define seasons. *Theor. Appl. Climatol.*, **38**, 57-68.
- Pielke, R. A., C-H. Yu, R. W. Arritt and M. Segal, 1984: Mesoscale air quality under stagnant conditions. *Air Pollution Effects on Parks and Wilderness Areas Conference*, Mesa Verde National Park, Colorado. Sponsored by the National Park Service.
- Raynor, G. S., J. V. Hayes and D. M. Lewis, 1983: Testing of the Air Resources Laboratories trajectory model on cases of pollen wet deposition after long-distance transport from known source regions. *Atmos. Environ.*, **17**, 213-220.
- Reisinger, L. M., and S. F. Mueller, 1983: Comparisons of tetroon and computed trajectories. *J. Climate Appl. Meteor.*, **22**, 664-672.
- Sheih, C. M., 1983: An evaluation of wind field interpolation schemes used in studies of regional-scale transport. *Trans. Air Pollution Control Association Specialty Conf. on the Meteorology of Acid Deposition*, P. J. Samson, Ed., Hartford, Air Pollution Control Association, 324-329.